

Potentiometric Study of a New Schiff Base and its Metal Ion Complexes: Preparation, Characterization and Biological Activity

Hamed M. Al-Saidi¹, Gamal A. Gouda^{2,*} and O. A. Farghaly²

¹ Chemistry Department, University College in Al-Jamoum, Umm Al-Qura University, 21955, Makkah, Saudi Arabia

² Faculty of Science, Al-Azhar University, Assiut Branch, 71524 Assiut, Egypt.

*E-mail: ggouda73@azhar.edu.eg

Received: 18 July 2020 / Accepted: 3 September 2020 / Published: 30 September 2020

Some metal complexes of a new Schiff base [4-(morpholin-4-yl)benzylidene]thiosemicarbazide (L) have been investigated. A potentiometric method was used to determine their stability constants by pH-metric titration. The stoichiometric protonation constants of L in 25 % (v/v) ethanol-water mixture and ionic strength of 1 mol dm⁻³ were found to be 4.88 and 10.21. The formation constants of the complexes increase in the order of La(III) > Fe(III) > Co(II) > Cu(II) > Mn(II) > Pd(II) > Ni(II) ions. The chemical structure of L and its metal complexes were established using elemental analyses and infrared spectroscopy. The microanalytical data reveals that a 1:1 (metal:ligand) stoichiometric ratio was found for the compounds. The geometric parameters of the metal-L complexes were assumed according to the density functional theory (DFT) method. The complexes show a moderate antibacterial inhibition against *Staphylococcus aureus* and *Escherichia coli* and a fair degree of antifungal activity against *Aspergillus fumigatus*, *Alternaria alternata* and *Fusarium oxysporum*.

Keywords: Potentiometric, new Schiff base, metal complexes, theoretical studies, antimicrobial activity.

1. INTRODUCTION

Thiosemicarbazone derivatives have received considerable attention in view of their variable bonding modes, ion-sensing ability, molecular structures and biological applications [1-4]. These derivatives are versatile chelators toward a range of metal ions, such as Cu(II), Zn(II), Pd(II), Co(III), Fe(III), Re(III), In(III), ect., with sulfur and azomethine nitrogen atoms [5]. The activity of these compounds is strongly dependent on the nature of the donor atoms N, S-didentate coordination mode [6, 7]. These have been studied extensively due to their sensitivity towards the central metal atom and

the occurrence of the imino group ($-\text{N}=\text{CH}-$), that imparts the biological activity [8-12]. Metal complexes of thiosemicarbazones have great medicinal importance and are reported to possess a wide variety of biological effects against fungi, bacteria, certain type of tumours and enzymatic inhibition [13-18]. In general, Cu(II), Zn(II), Cd(II) and Hg(II) have the greatest binding power with nitrogen and sulfur ligands of any of the metal ions [19-20].

The aims of this research are to determine the formation and equilibrium constants of [4-(morpholin-4-yl)benzylidenyl]thiosemicarbazide and its Mn(II), Fe(III), Co(II), Ni(II), Cu(II), Pd(II) and La(III) ion complexes by the potentiometric titration method, employing ethanol-water medium at an ionic strength of 1 mol dm^{-3} adjusted by the addition of NaClO_4 . The physicochemical properties of the synthesized ligand-metal complexes will be investigated by different analytical techniques. The project is a comprehensive study with a conclusion based on data obtained for the electronic and biological applications of the obtained ligand-metal complexes.

2. EXPERIMENTAL

2.1. Physical measurements

The reagents used in the present work were weighed on a Sartorius balance. All pH-metric titrations were carried out at $25 \text{ }^\circ\text{C}$ using a Misura Line 1010 pH meter (Romania) equipped with a combined porolyte electrode and stirred by a heated magnetic stirrer (VELP Scientifica) during the experimental procedures. In addition, a micropipette ($100\text{-}1000 \text{ }\mu\text{L}$) was also used. The concentrations of carbon, hydrogen, nitrogen, and sulfur in the prepared compounds were determined by an Elementar Analysensysteme GmbH Vario El analyzer. Mass spectra were recorded by a JEOL JMS 600 spectrometer at an ionizing potential of 70 eV using the direct inlet system. Infrared spectra of the compounds were obtained in the $4000 \text{ to } 400 \text{ cm}^{-1}$ region with a Nicolet model 6700 spectrophotometer using the KBr disc technique. The proton nuclear magnetic resonance was determined by a Varian EM390 spectrophotometer. Conductance measurements were recorded by using a model 4320 Conductivity Meter. The distribution diagrams were drawn in the titration where the metal ions to ligand, mole ratio was 1:1, 1:2 and 1:3 in aqueous solution at $25 \text{ }^\circ\text{C}$ and an ionic strength of $\mu = 1 \text{ mol dm}^{-3} \text{ NaClO}_4$. It was obtained using Microsoft Excel calculations.

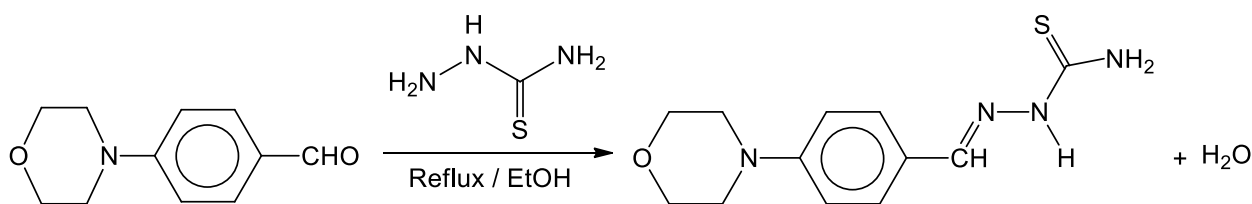
2.2. Potentiometric studies of L and its metal complexes

In aqueous solution, three titrations were performed for the determination of the formation constants of L and its metal complexes at $25 \pm 1 \text{ }^\circ\text{C}$. The solutions were titrated potentiometrically using standard sodium hydroxide solution (0.2 mol dm^{-3}) standardized against standard potassium hydrogen phthalate, $\text{C}_8\text{H}_5\text{KO}_4$, [21, 22]. Metal ion solutions of Cu(II), Fe(III), Co(II), Mn(II), Pd(II), Ni(II), and La(III) were prepared using deionized water and determined by EDTA [23]. The total volume was completed to 50 mL adding ethanol and deionized water in each case to obtain a $25 \text{ } \%$ (v/v) ethanol-water mixture. The titrations were performed at ionic strengths of $\mu = 1 \text{ mol dm}^{-3} \text{ NaClO}_4$. The

following mixtures were prepared and titrated against a standard solution of 0.2 mol dm^{-3} NaOH. Titrations of the following mixtures were carried out: (i) 5 mL of 0.1 mol dm^{-3} HClO₄, (ii) Solution (i) + 5 mL of L ligand ($10^{-2} \text{ mol dm}^{-3}$), and (iii) Solution (ii) + 10 mL ($10^{-3} \text{ mol dm}^{-3}$) of the metal salt under investigation in a total of 50 mL ethanol-water mixture. The pH measurements were carried out using a KF and potentiometric titrator described in experimental part and at a constant ionic strength greater than that of the metal ion concentration.

2.3. Preparation of [4-(morpholin-4-yl)benzylidenyl]thiosemicarbazide

A new Schiff base, [4-(morpholin-4-yl)benzylidenyl]thiosemicarbazide was synthesized by condensation of equal amounts of 4-morpholinobenzaldehyde and thiosemicarbazide in 50 mL ethanol. The synthetic route is outlined in Scheme 1. The product in its solid state was collected by filtration and recrystallized from ethanol as red crystals; yield 85 %; m.p. 270 °C.



Scheme 1. Synthesis of [4-(morpholin-4-yl)benzylidenyl]thiosemicarbazide.

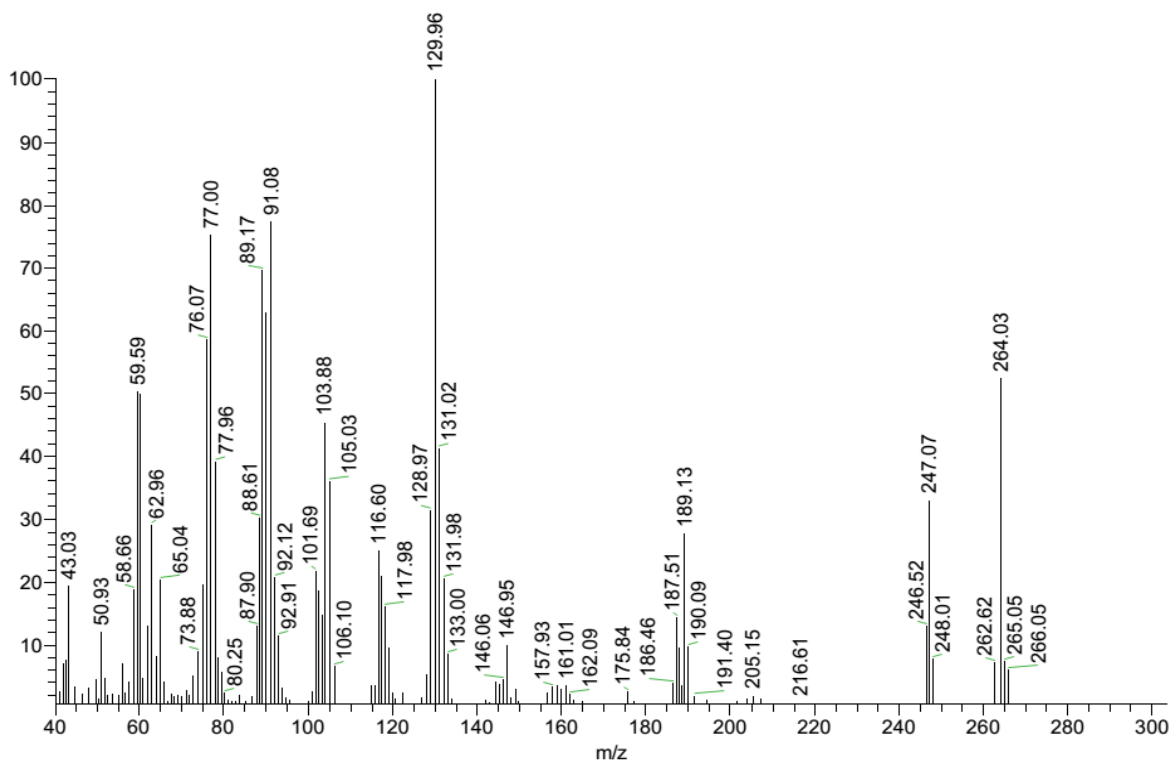


Figure 1. Mass spectrum of L.

The fragmentation pathway of L (Fig. 1), is characterized by the appearance of molecular ion peaks at m/z : 264.03 (52.29 %), at m/z : 189.13 (27.78 %) for $[M-C_{11}H_{13}ON_2]^+$, and at m/z : 187.51 (14.14 %) for $[M-C_6H_4]^+$ with a base peak at m/z : 129.96 (100 %), [24]. The 1H NMR spectrum ($CDCl_3$) of L revealed the appearance of protons at δ (ppm): 3.30 [m, 4H, $N(CH_2)_2$], 3.25-3.78 (m, 4H, Ar-H) and 6.80-7.80 (s, 1H, $CH=N$) which supports the structure.

2.4. Preparation of binary solid complexes

A heated methanolic solution of a suitable amount of L was mixed with a weighted amount of the respective metal salt (iron(III), manganese(II), nickel(II), copper(II), palladium(II) and lanthanum(III) chlorides) dissolved in alcohol with molar ratios of 1:1. The mixture was then stirred for about three hours. The solid complexes were obtained by the addition of ether and then filtered immediately. The complexes were then filtered off, washed and dried over P_2O_5 .

2.5. Biological activity

Antimicrobial Assay: The agar well diffusion method was used to detect the antimicrobial activities of the tested chemical compounds [25]. Solutions of 0.05 g of each compound in 1 mL of dimethyl sulfoxide as a solvent were prepared. The plates were poured with 20 mL NA medium for bacteria and PDA medium for fungi. Wells 7 mm in diameter were cut into these agar plates and 100 μ L of the mixture was placed into each well. The bacterial culture plates were incubated at 37 °C for 24 hours and fungal culture plates were incubated at 28 °C for 5-7 days. The diameters of the zones of inhibition were measured (mm). All the bacterial and fungal cultures were provided by the National Committee for Clinical Laboratory Standards (NCCLS), Assiut, Egypt.

3. RESULTS AND DISCUSSION

3.1. Acid-base equilibrium of [4-(morpholin-4-yl)benzylidenyl]- thiosemicarbazide

The formation constants of L were determined in the absence and presence of metal ions and at a constant ionic strength greater than that of the metal ion concentration under investigation. The calculations were performed on the data points in each titration using the *Excel* computer program [26-28]. The equilibrium constant (\bar{n}_A) of each ligand under experimental conditions was determined by a Calvin pH-metric titration as modified by Irving and Rossotti [29, 30] (1).

$$\bar{n}_A = Y + \frac{(V_1 - V_2)(N^\circ + E^\circ)}{(V^\circ + V_1)TC_L^\circ} \quad (1)$$

where Y is the total number of dissociable protons attached to the ligand molecule (here equal to 1), V_1 and V_2 are the volumes of sodium hydroxide (mL) necessary to reach the same pH in acid and ligand titration curves, respectively, N° is the concentration of alkali, E° is the initial

concentration of free acid, V° is the initial volume of the mixtures (50 mL), and TC_L° is the concentration of ligand in the 50 mL of solution. The acid dissociation of the metal complexes under study is calculated from the titration curves of HClO_4 with NaOH in the absence and in the presence of the ligand. Different behaviours in the titration curves are obtained as shown in Figure 2 where the observed pH was plotted against the volume of alkali. The titration curves reveal that the magnitude of the horizontal displacement of the complexes curves (c-i) from the free L is greater with the metal ions.

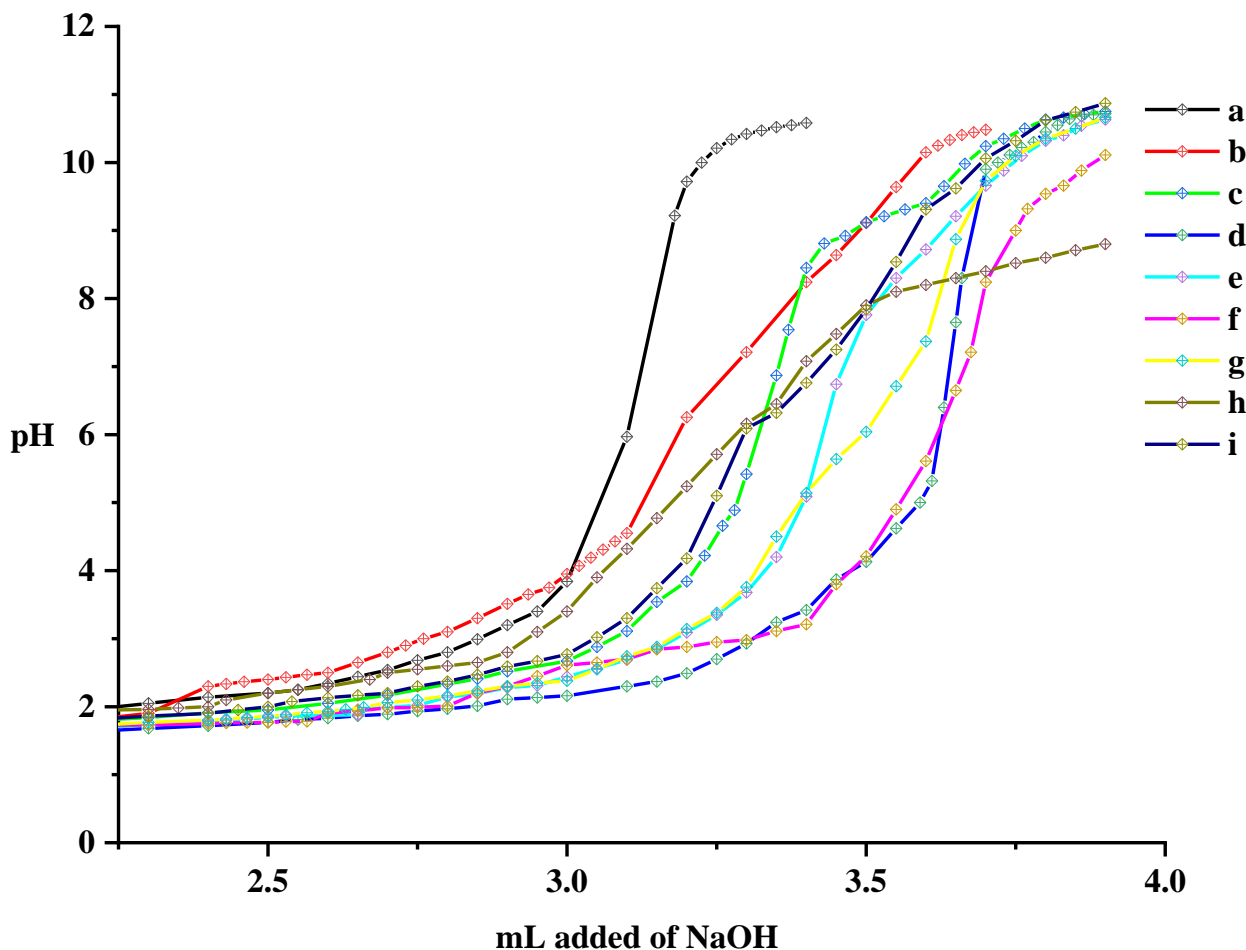


Figure 2. Titration curves of L with different metal ions in $\mu = 1 \text{ mol dm}^{-3}$ NaClO_4 (25 % (v/v) ethanol-water mixture). (a): HClO_4 , (b): $\text{HClO}_4 + \text{L}$, (c): b + Mn(II) , (d): b + Fe(III) , (e): b + Co(II) , (f): b + Ni(II) , (g): b + Cu(II) , (h): b + Pd(II) and (i): b + La(III) ions.

Practically, it is observed that the Mn^{II} -complex (curve c) begins to form at a lower pH value (2.02) than the Co^{II} -complex (curve e) (2.83). Precipitation began at $\text{pH} > 10$, therefore, no calculations could be carried out after this point, where the hydroxide species likely to be formed after the precipitation could not be studied. The formation curve was obtained by plotting the values of \bar{n}_A against the pH values of the L (Fig. 3).

L has an acidic character (higher pK_H value), according to the values of pK_{NH} , which is found to be 10.21. The pK_{NH} value is due to the deprotonation of an imino group [31-33], while a higher acidic property according to the pK_{NH_2} value (4.88) is due to the protonation of an amino group [34, 35].

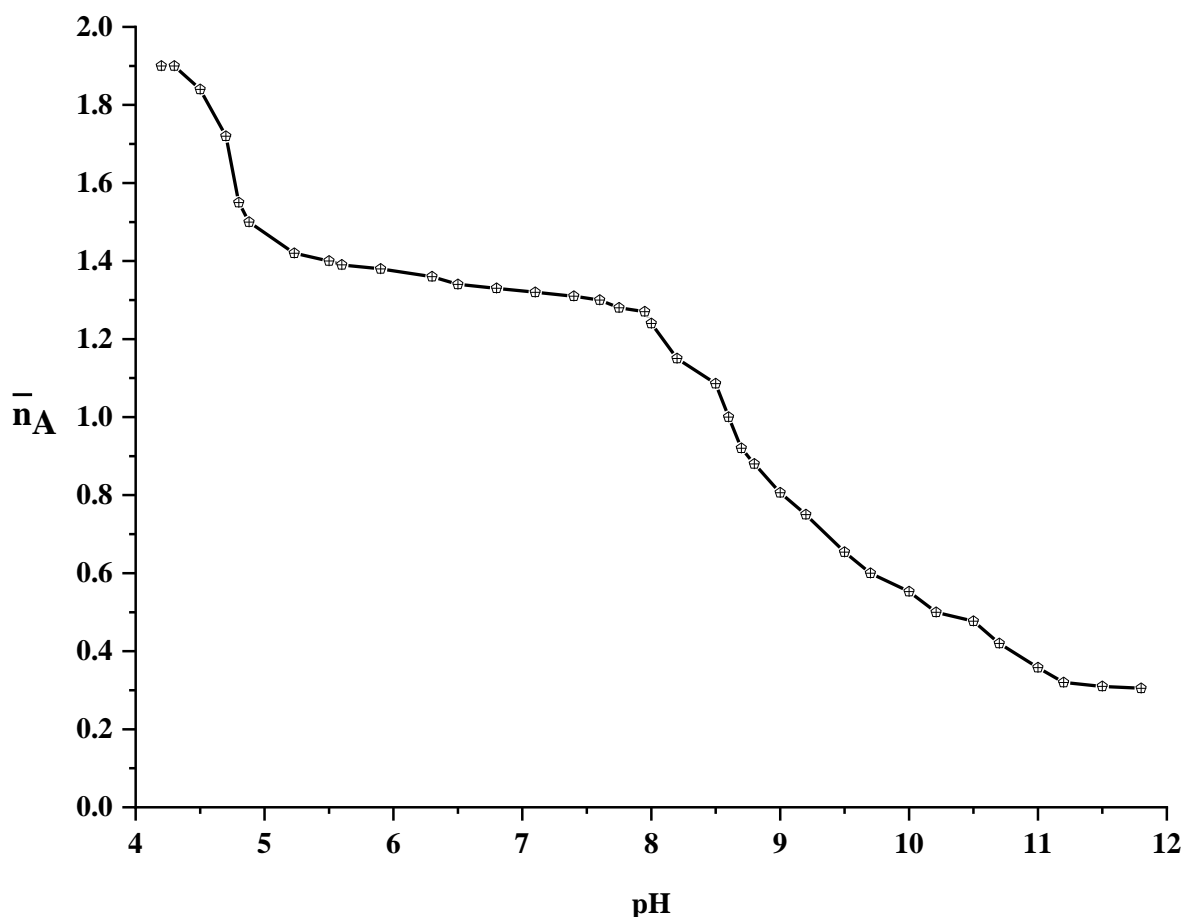
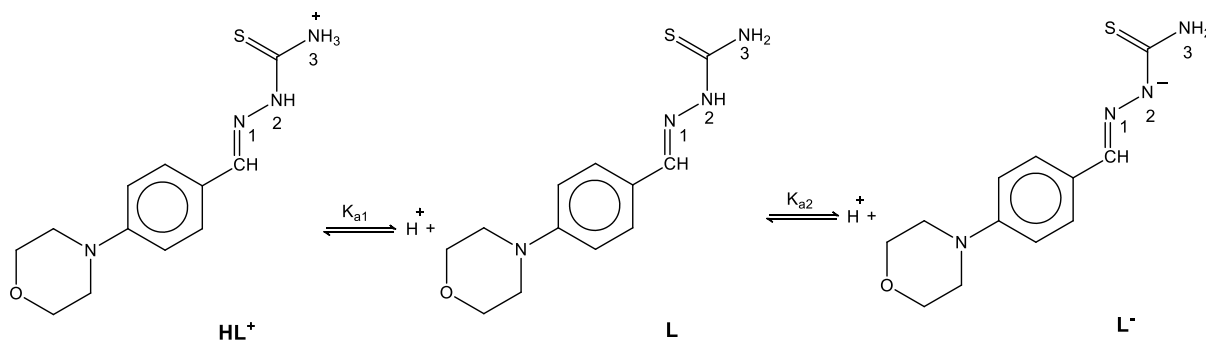


Figure 3. Formation curve of L plotting \bar{n}_A against different pH values in $\mu = 1 \text{ mol dm}^{-3} \text{ NaClO}_4$.

The molecular form L ionizes in a cationic form, HL^+ as the pH decreases and converts to an anionic form, L^- when increasing the pH. Scheme 2 shows the pathway of two-step dissociation of L, where K_{a1} and K_{a2} are the protonation and deprotonation constants of the N2 and N3 atoms, respectively.



Scheme 2. The protonation and deprotonation sites of L.

3.2. Stability constants of binary metal complexes

It is clear that the pH-metric titration curves of the metal salts, viz, Ni(II), Cu(II), Pd(II), Fe(III), Co(II), Mn(II), and La(III) with L are well separated from the ligand titration curve. Consequently, the replacement of hydrogen ion is because of complexation. The stability constants of metal-L complexes were obtained from the curves (Fig. 4) drawn between the formation functions \bar{n} and pL values, which can be computed from equations 2 and 3 using the half method [29, 30].

$$\bar{n} = \frac{(V_3 - V_2)(N^\circ + E^\circ)}{(V^\circ + V_2)\bar{n}_A T C_M^\circ} \quad (2)$$

$$pL = \log \frac{\sum_{n=0}^{n=i} \beta_n^H \left(\frac{1}{\text{anti log } pH}\right)^n}{T C_L^\circ - \bar{n} T C_M^\circ} \cdot \frac{V^\circ + V_3}{V^\circ} \quad (3)$$

where V_3 is the alkali volume employed to arrive at the same pH value, $T C_M^\circ$ is the total amount of metal ion found in the titration solution, while, β_n^H is the overall stability constant (4).

$$\log \beta = \log K_{ML}^M + \log K_{ML_2}^M + \log K_{ML_3}^M \quad (4)$$

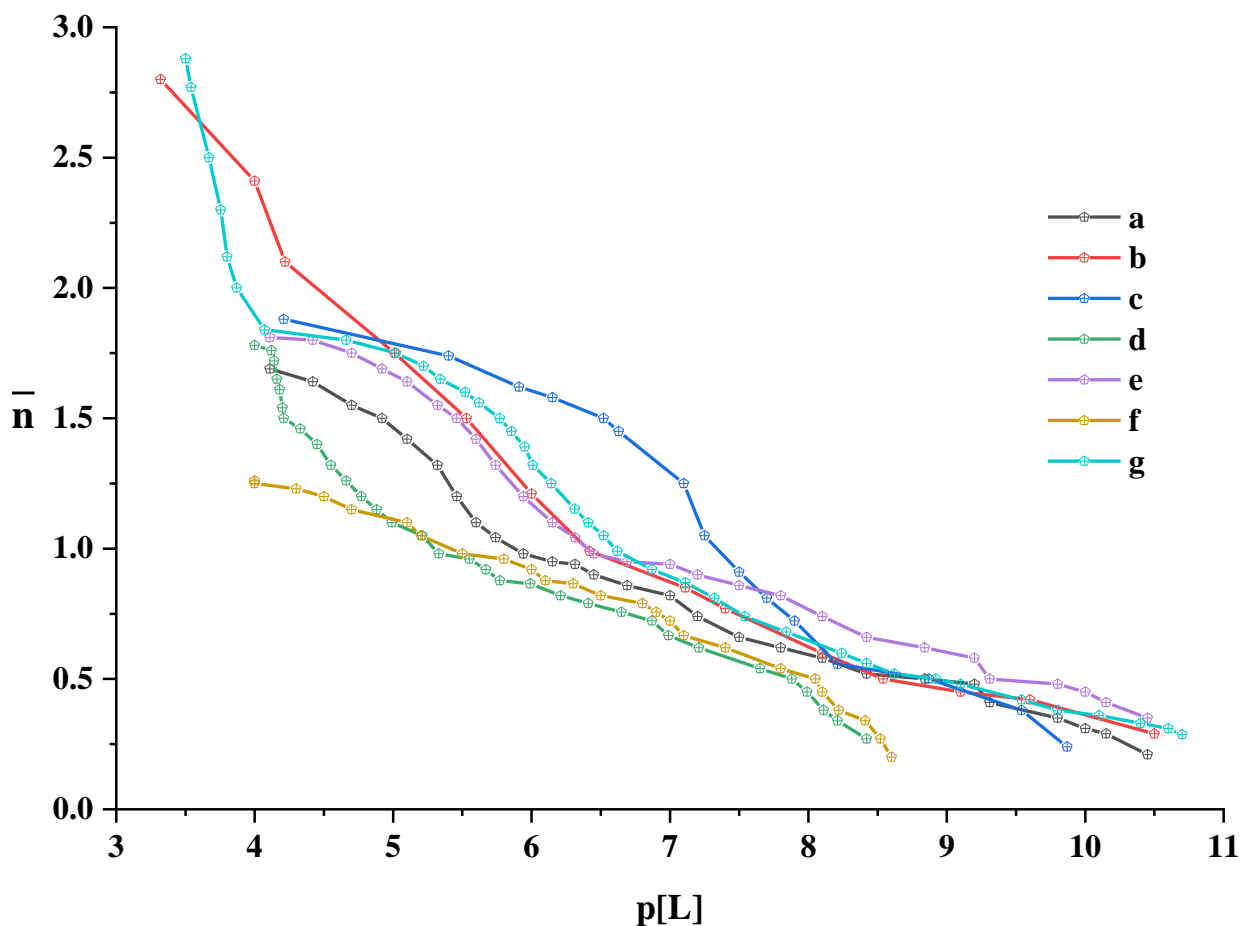


Figure 4. Formation curves of metal ion complexes with L, (a) Mn^{II} -L (b) Fe^{III} -L, (c) Co^{II} -L, (d) Ni^{II} -L, (e) Cu^{II} -L, (f) Pd^{II} -L and (g) La^{III} -L species.

The formation curves are indicative of the species M:L present at ratios of 1:1, 1:2 and 1:3. The following general observations can be made: (i) these are the important types of species due to the presence of three inflections in the case of the 1:1, 1:2 and 1:3 species after the addition of 3 moles of sodium hydroxide per 1 mole of L [36]. (ii) The metal solutions employed in the present investigation are dilute (2×10^{-4} mol dm⁻³); Thus, under these conditions, the possibility of the formation of polynuclear complexes is low [37]. (iii) The metal ion titration curves were shifted to the right-hand side of the ligand titration curve along the volume axis, referring to proton release upon formation of the metal ions complexes with the ligand. (iv) A change in colour from yellow to brown, black or red in the pH range of 3-10 over titration indicated the formation of a complex between metal and ligand. The large decrease in pH for the metal titration curves compared to the ligand titration curve implies to the strong metal complexes formation [38]. The overall formation constants of binary systems have been compared using standard methods dependent on the calculation of the average number of ligands bound per metal ion [39, 40]. The dissociation constants in addition to the stability constants ($\log K_i$) of the complexes of L with metal ions under investigation have been evaluated at 25 ± 1 °C and the values are listed in Table 1.

Table 1. Formation constants of metal-L complexes in 25 % (v/v) ethanol-water mixture

Species	$\log K_1$	$\log K_2$	$\log K_3$	$\log \beta$
L	4.88 (4.95)*	10.21 (10.37)*	-	14.09 (15.32)*
Mn ^{II} -L	8.84	4.92	-	13.76
Fe ^{III} -L	8.54	5.53	3.66	17.73
Co ^{II} -L	8.87	6.52	-	15.39
Ni ^{II} -L	7.88	4.21	-	12.09
Cu ^{II} -L	9.31	5.46	-	14.77
Pd ^{II} -L	8.05	-	-	8.05
La ^{III} -L	8.92	7.77	3.67	20.36

* Point-wise method

In the present study, the formation constants of the complexes of metal ion with L obeyed this order: La(III) > Fe(III) > Co(II) > Cu(II) > Mn(II) > Pd(II) > Ni(II). The order of stability constants of the binary complexes formed between L ligand and transition metal ions investigated in this study is in the expected Irving-Williams series [41, 42] for 1:1 and 1:2 ratios of metal to ligand. The greater stability of the La^{III}-L system is most likely attributed to the Jahn-Teller effect [43, 44]. Additionally, the high stability of Fe^{III}-L and La^{III}-L species can best be viewed in light of the observation that Fe(III) and La(III) are hard Lewis acids with a high charge [45].

3.3. The distribution diagrams

The dissociation constants of L in addition to the stability constants of its complexes with some metal ions were used to plot the distribution curves for the formed species in aqueous solution at 25 °C

and an ionic strength of $\mu = 1 \text{ mol dm}^{-3} \text{ NaClO}_4$ [46, 47]. It was obtained using Microsoft Excel calculations and the concentration of total metal ions $2 \times 10^{-4} \text{ mol dm}^{-3}$ was set as 100% [48].

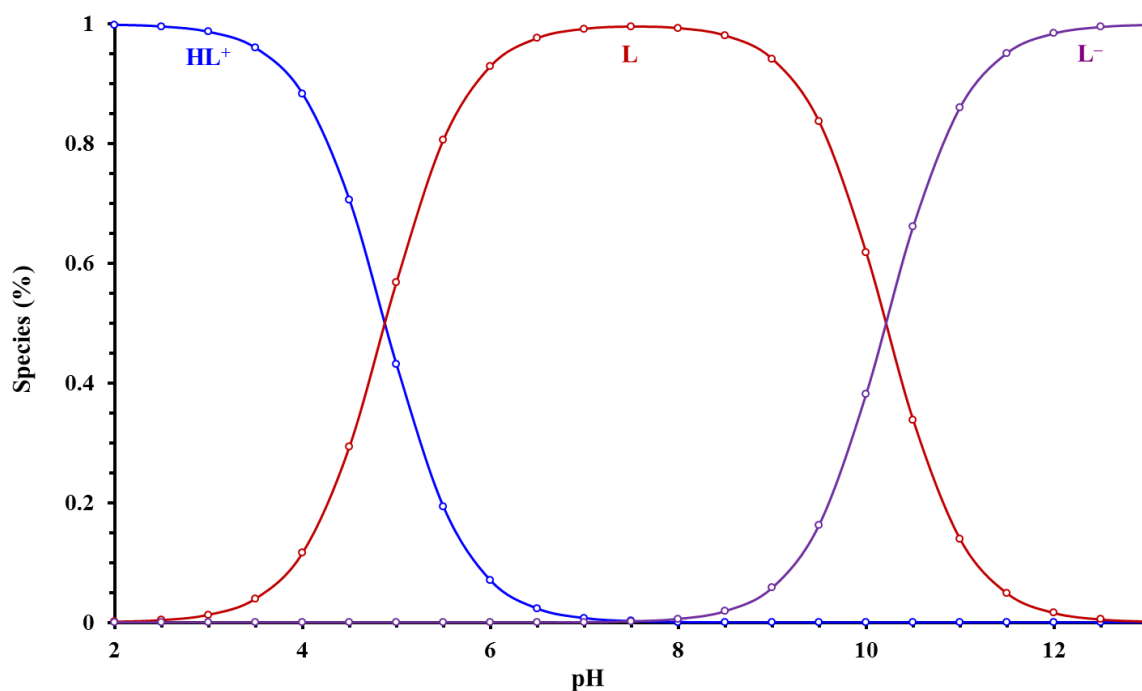


Figure 5. The fractional composition of the protonation and deprotonation forms of L in aqueous solution as a function of pH.

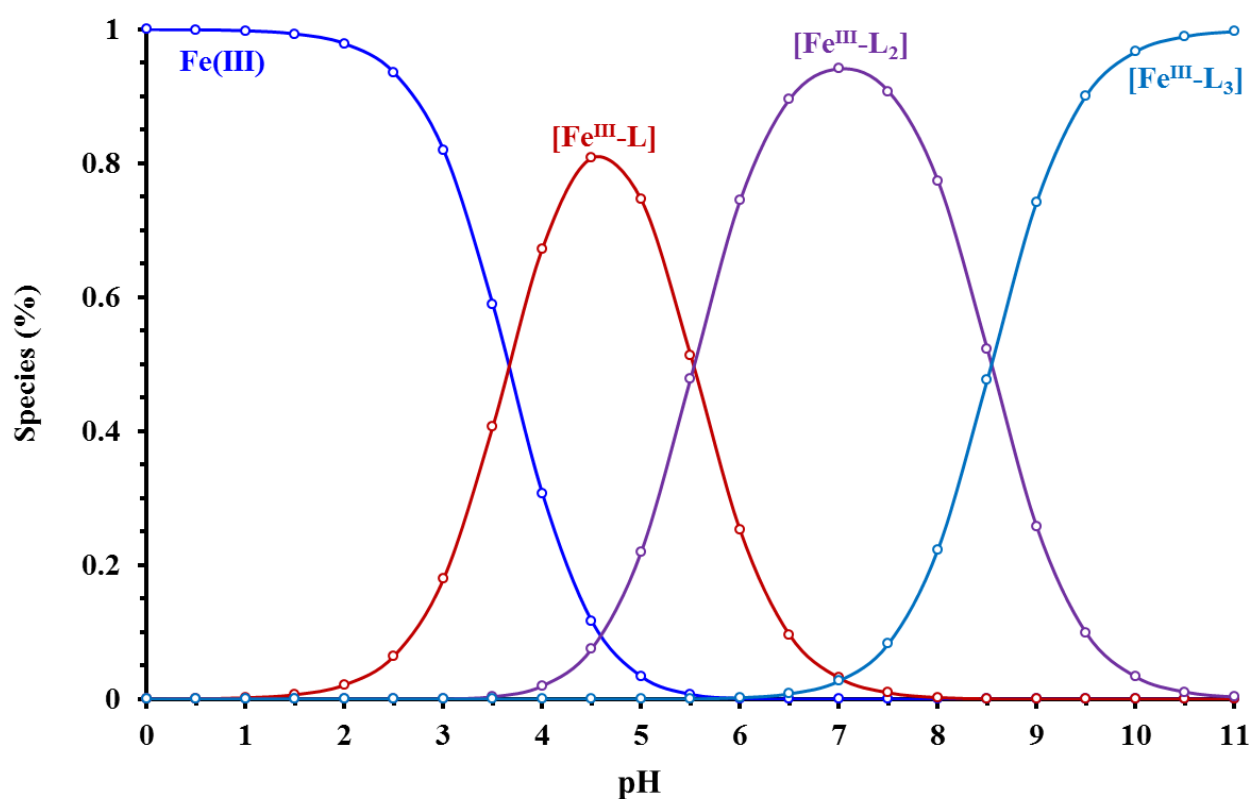


Figure 6. Distribution curves of the various forms of the $\text{Fe}^{\text{III}}\text{-L}$ complexes.

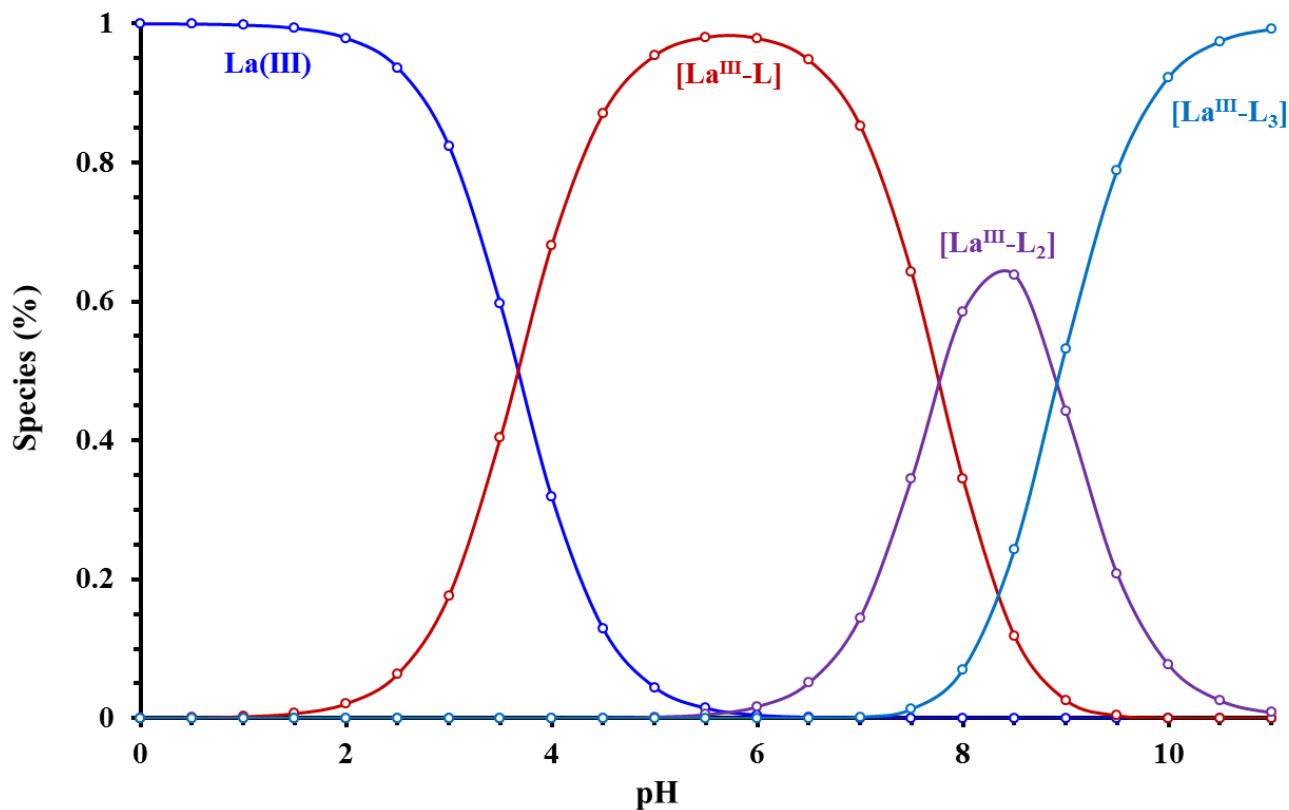


Figure 7. Distribution curves of the various forms of the La^{III}-L complexes.

The concentration distribution diagrams of the L, Fe^{III}-L and La^{III}-L species as representatives are shown in Figures 5-7, respectively. In acidic solution (pH < 5), L initially exists in the fully protonated form as HL⁺. With increasing the pH, the species L loses one proton forming L⁻, which is the highly predominant species at pH 10.22. At pH values below 5.5, the Fe^{III}-L species are formed with a lesser amount (80.08 %). In contrast, a very high amount of the [Fe^{III}-L₂] species is formed (94.09 %). Therefore, L reacts with Fe(III) selectively in the acidic and basic ranges. A high amount of the La^{III}-L system is formed at pH 5.8, but a lesser amount of the [La^{III}-L₂] system is formed (65%).

3.4. Characterization of the isolated solid complexes

The interaction of Mn(II), Ni(II), Cu(II) and Pd(II) ions with L results in the formation of [MCl₂L]·nH₂O (where M = Mn(II), Ni(II), Cu(II) or Pd(II) and n = 4, 5, 1 or 3, respectively). The chemical structures of complexes formed between L ligand and Mn(II), Ni(II), Cu(II) and Pd(II) ions were confirmed by IR, elemental analyses, and molar conductivity.

The resulting complexes are partially soluble in ethanol, but completely soluble in dimethyl sulfoxide, acetone, and dimethyl formamide (DMF). The molar conductivity of the obtained complexes in DMF solution (10⁻⁴ mol L⁻¹) was measured at room temperature, which suggests the non-electrolytic nature of these complexes [49, 50]. The physical characterizes of and analytical data for these complexes are tabulated in Table 2.

Table 2. The formulas, molecular weights, colours, molar conductance and elemental analysis results of L and its metal complexes

Compounds	Mol. wt. (g mol ⁻¹)	Colour	Conductivity (mS/cm)	Calculated (Found) %			
				C	H	N	S
L	264.34	Yellow	-	54.47 (54.46)	6.05 (6.15)	21.18 (21.13)	12.10 (12.14)
[MnCl ₂ L]·4H ₂ O	462.04	Light yellow	2.80	31.16 (31.36)	5.19 (5.21)	12.12 (12.25)	6.92 (6.98)
[NiCl ₂ L]·5H ₂ O	483.85	Gold	2.43	29.76 (31.48)	5.37 (5.40)	11.57 (11.62)	6.61 (6.65)
[CuCl ₂ L]·H ₂ O	416.78	Reddish brown	3.19	34.55 (34.60)	4.32 (4.33)	13.43 (13.48)	7.68 (7.72)
[PdCl ₂ L]·3H ₂ O	495.64	Brown	3.87	29.05 (30.01)	4.44 (4.50)	11.30 (11.39)	6.46 (6.50)

The most important IR spectral bands of L and its metal complexes are listed in Table 3 and are illustrated in Figure 8. In the IR spectrum of L, a sharp band is located at 1589 cm⁻¹ that is assigned to the stretching mode of C=N- group. This band shifts to a lower wavenumber by 6-26 cm⁻¹ after complexation except for the Mn^{II}-L compound, where the band was observed at a higher wavenumber by 9 cm⁻¹.

Table 3. Characteristic infrared spectral bands of the L and their metal complexes (ν/cm⁻¹)

Compounds	ν(N-H)	ν(C=N)	ν(C=S)	ν(M-S)	ν(M-N)
L	3161	1609	824	-	-
[MnCl ₂ L]·4H ₂ O	3172	1598	790	495	535
[NiCl ₂ L]·5H ₂ O	3172	1541	789	487	535
[CuCl ₂ L]·H ₂ O	3173	1557	772	490	508
[PdCl ₂ L]·3H ₂ O	3171	1551	750	480	530

These shifts indicate the coordination of azomethine group to a metal ion [51, 52]. The frequencies of C=N- group in IR spectra of metal complexes are listed in Table 3. The ν(S-H) band at 2565 cm⁻¹ is absent in the IR spectrum of the ligand, whereas, the ν(N-H) band at 3161 cm⁻¹ is clearly observed. This indicates that ligand remains as the thionic tautomer in its solid state [53, 54]. The ν(C=S) bands observed around 750 to 824 cm⁻¹ in the spectrum of the ligand have been shifted to lower frequencies by 24 to 58 cm⁻¹ after complexation [55]. This is a result of the coordination of the sulfur atom of the C=S group. In all complexes, the coordination is confirmed by the presence of two

bands in the regions of 480 to 495 cm^{-1} and 508 to 535 cm^{-1} . These can be assigned to the $\nu(\text{M-S})$ and (M-N) bonds, respectively [56-58]. The stretching vibration of the $\nu(\text{NH})$ group is observed in the range 3161 to 3174 cm^{-1} and no shift of the frequency of this group was observed upon complexation to the ligand. This excludes the coordination of (NH) group to the metal ions [59]. According to the above experimental results, the chemical structure of the complexes prepared in the present study is shown in Figure 9.

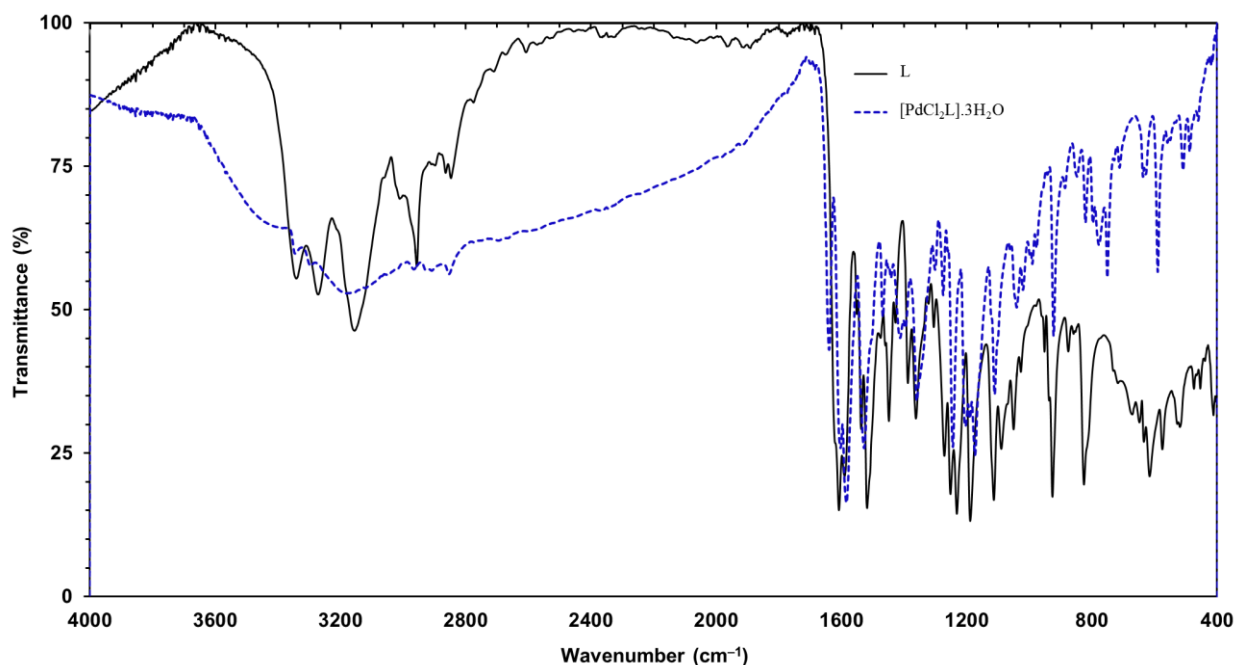


Figure 8. The IR spectra of the L and $[\text{PdCl}_2\text{L}] \cdot 3\text{H}_2\text{O}$ complex.

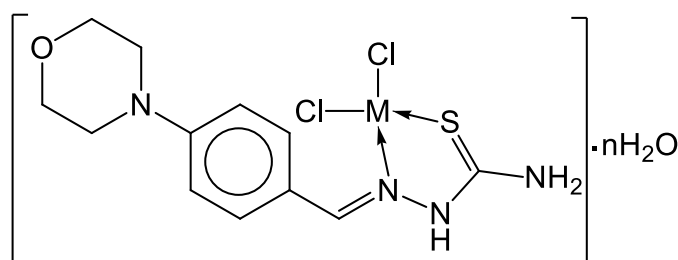


Figure 9. The proposed chemical structures of the metal complex of L (where $\text{M} = \text{Pd}(\text{II})$, $\text{Ni}(\text{II})$, $\text{Cu}(\text{II})$, or $\text{Mn}(\text{II})$, and $n = 3, 5, 1$ or 4 respectively).

3.5. Quantum chemical calculations

The geometrically optimized structures of the synthesized complexes was obtained using quantum chemical calculations. Optimization of geometries was performed by the density functional theory method (DFT) using the Gaussian 09 program package since DFT methods are very effective in modelling compounds [60, 61]. Some parameters of the quantum calculation such as E_{Homo} , E_{Lumo} ,

energy gap (E_g), ionization potential (I) and electron affinity (A) are given in the following relations (5-7):

$$A = -E_{\text{Lumo}} \quad (5)$$

$$I = -E_{\text{Homo}} \quad (6)$$

$$E_g = E_{\text{Lumo}} - E_{\text{Homo}} \quad (7)$$

The order of stability of the metal-L complexes is Pd(II) > Ni(II) > Mn(II) > Cu(II) as a result of the values of the energy gap between E_{Homo} and E_{Lumo} (Table 4). The Pd^{II}-L complex has a higher energy gap than those of the other metal complexes. A low value of the energy bond gap of the Cu^{II}-L system produces greater activity (less stability), because the energy required to remove an electron from the last occupied orbital will be low [62]. The molecular properties of the optimized geometry of some metal complexes (1:1 ratio) are shown in Figures 10 and 11.

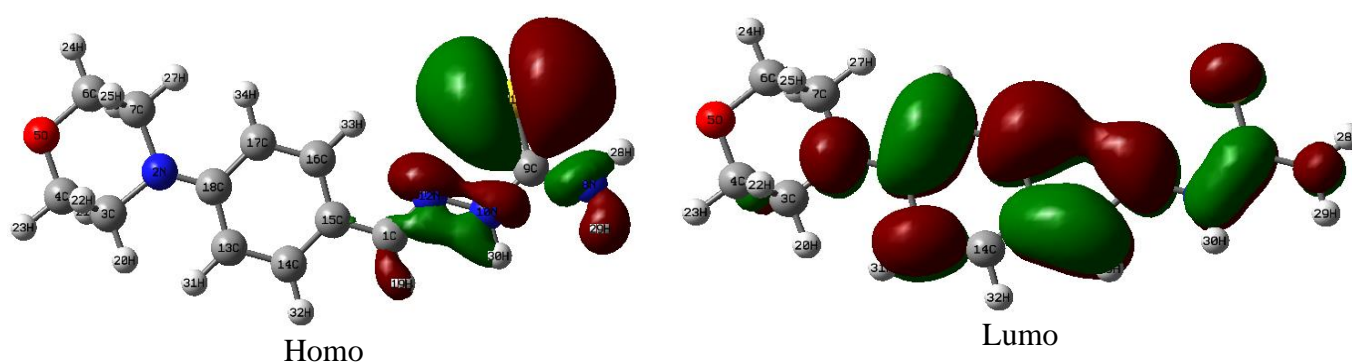


Figure 10. Calculated high spin (E_{Homo}) and low spin (E_{Lumo}) molecular orbitals of L using the B3LYP/6-311++G(d,p) method.

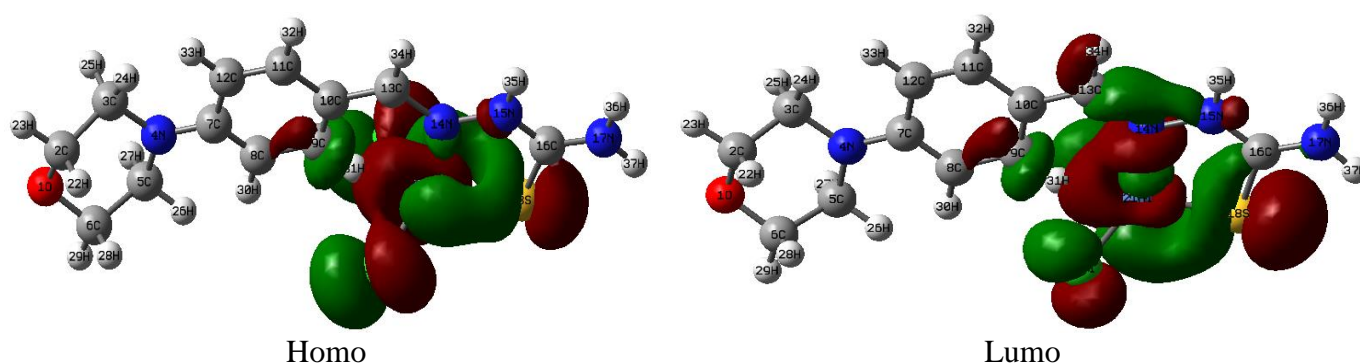


Figure 11. Calculated high spin (E_{Homo}) and low spin (E_{Lumo}) molecular orbitals of the $[\text{NiCl}_2\text{L}] \cdot 5\text{H}_2\text{O}$ complex using the B3LYP/6-311++G(d,p) method.

Table 4. The molecular properties of metal-L complexes calculated with the DFT (B3LYP) level of theory using the standard basis 6-311G ++ (d,p)

Compounds	E _{Homo} (ev)	E _{Lumo} (ev)	E _g (ev)	I	A
L	-0.27462	-0.19804	0.07658	0.27462	0.19804
[MnCl ₂ L]·4H ₂ O	-0.23766	-0.22740	0.01026	0.23766	0.22740
[NiCl ₂ L]·5H ₂ O	-0.23065	-0.21777	0.01288	0.23065	0.21777
[CuCl ₂ L]·H ₂ O	-0.18863	-0.18075	0.00790	0.18863	0.18075
[PdCl ₂ L]·3H ₂ O	-0.20458	-0.15078	0.05380	0.20458	0.15078

3.6. The biological activity of the synthesized compounds

The antibacterial activities of the free ligand and its complexes were tested against some strains of bacteria and fungi; namely, *Bacillus cereus* (G +ve), *Staphylococcus aureus* (G +ve), *Escherichia coli* (G -ve), *Pseudomonas aeruginosa* (G -ve), *Aspergillus niger*, *Aspergillus flavus*, *Aspergillus fumigatus*, *Alternaria alternata*, *Fusarium oxysporum* and *Candida albicans* were used as antibacterial and antifungal standards, respectively. Table 5 summarizes the antimicrobial activities of the prepared compounds. It was observed that the activity of L is not effective against all the bacteria undertaken in the present study. The [NiCl₂L]·5H₂O complex is not effective against all the fungi, however, this complex was proved to be an excellent candidate as an antibacterial agent, with the ability to inhibit all bacterial species. In addition, the [CuCl₂L]·H₂O complex is more effective against *Bacillus subtilis* and *Pseudomonas aeruginosa* than against *Staphylococcus aureus* or *Escherichia coli*. Similarly, *Aspergillus niger* and *Aspergillus flavus* were highly susceptible to [CuCl₂L]·H₂O and [PdCl₂L]·3H₂O but less susceptible to [MnCl₂L]·4H₂O and [NiCl₂L]·5H₂O.

Table 5. The antibacterial and antifungal activities of the prepared compounds (Tested bacterial strains, a zone of inhibition in mm)*

Species	Compounds				
	L	[MnCl ₂ L]·4H ₂ O	[NiCl ₂ L]·5H ₂ O	[CuCl ₂ L]·H ₂ O	[PdCl ₂ L]·3H ₂ O
<i>B. subtilis</i>	-ve	2.7	3.2	3.0	2.4
<i>S. aureus</i>	-ve	1.9	2.8	2.0	2.3
<i>E. coli</i>	-ve	2.0	2.5	2.1	1.8
<i>P. aeruginosa</i>	-ve	1.6	3.2	3.0	1.8
<i>A. niger</i>	1.8	1.9	-ve	2.5	2.1
<i>A. flavus</i>	-ve	1.6	-ve	1.8	1.9
<i>A. fumigatus</i>	-ve	-ve	-ve	-ve	1.7
<i>A. alternata</i>	-ve	-ve	-ve	-ve	-ve
<i>C. albicans</i>	-ve	2.00	-ve	1.6	2.00
<i>F. oxysporum</i>	-ve	-ve	-ve	-ve	-ve

*Notes: 4-3: Strong inhibition, 3-2: moderate inhibition, 2-1: weak inhibition, (-ve): no inhibition

4. CONCLUSION

A new ligand, [4-(morpholin-4-yl)benzylidene]thiosemicarbazide and its metal complexes were prepared and characterized using different techniques e.g. elemental analysis, ^1H NMR, FT-IR and MS. The potentiometric studies of the ligand complexes with Fe(III), Mn(II), Ni(II), Co(II), Cu(II), Pd(II) and La(III) ion were carried out in 25 % (v/v) ethanol-water mixture at an ionic strength of $1 \text{ mol dm}^{-3} \text{ NaClO}_4$. The stability constants of the ligand complexes with metal ions under study were calculated and discussed in detail. The ligand has a lower acidic character according to its value of pK_{NH} , which is found to be 10.21. The pK_{NH} value is due to the deprotonation of the imino group. In contrast, a higher acidic property according to the pK_{NH_2} value of 4.88 is due to the protonation of an amino group. The stoichiometry of the binary complexes suggested that the ligand forms 1:1, 1:2 and 1:3 ratios of binary complexes. The formation constants of the metal ion complexes with the ligand obeyed this order: $\text{La(III)} > \text{Fe(III)} > \text{Co(II)} > \text{Cu(II)} > \text{Mn(II)} > \text{Pd(II)} > \text{Ni(II)}$. The order of stability constants of the binary complexes formed between the ligand and the metal ions selected in this study are in the expected Irving-Williams series, for the 1:1 and 1:2 ratios of metal to ligand. The greater stability of $\text{La}^{\text{III}}\text{-L}$ system is due to Jahn-Teller effect. Additionally, the high stability of Fe(III) and La(III) complexes with L can best be viewed in light of the observation that Fe(III) and La(III) are hard Lewis acids with a high charge. The stoichiometry of the resulting binary complexes could be obtained from the elemental analysis, namely, ratios of 1:1 and 1:2. The molar conductance for all the complexes in 10^{-4} molar solution in pure DMF are ($\Lambda_{\text{M}} = 2.43\text{--}3.87 \text{ mS/cm}$) which suggest the non-electrolytic nature of these complexes. From the study of IR spectra, we can conclude that the ligand serves as a neutral bidentate ligand and coordinates to the metal ions via the azomethine nitrogen and sulfur atoms. The $\text{Pd}^{\text{II}}\text{-L}$ system has an energy gap higher than those of the other metal complexes. The low value of the energy gap of $\text{Cu}^{\text{II}}\text{-L}$ species produces greater activity and less stability because the removal energy of an electron from the last occupied orbital will be low. The biocidal activity of the obtained compounds was examined against gram-positive and gram-negative bacteria as well as against filamentous fungi. The complex of $[\text{CuCl}_2\text{L}]\cdot\text{H}_2\text{O}$ is more effective against *Bacillus subtilis* and *Pseudomonas aeruginosa* than against *Staphylococcus aureus* or *Escherichia coli*.

References

1. D. Mishra, S. Naskar, M. G. B. Drew and S. K. Chattopadhyay, *Inorg. Chim. Acta*, 359 (2006) 585–592.
2. H. A. El-Masry, H. H. Fahmy and S. H. A. Abdelwahed, *Molecules*, 5 (2000) 1429–1438.
3. J. S. Casas, M. S. García-Tasende and J. Sordo, *Coord. Chem. Rev.*, 209 (2000) 197–261.
4. R. G. Brown and J. Alan, *J. Chem. Soc., Perkin Trans.*, 1 (1987) 547–551.
5. R. Tudor, G. Aurelian, N. Anca and G. Rodica, *Molecules*, 12 (2007) 782–796.
6. R. V. Singh, N. Fahmi and M. K. Biyala, *J. Iran. Chem. Soc.*, 2 (2005) 40–46.
7. M. Belicchi-Ferrai, F. Biscegli, G. Pelosi, S. Pinelli and P. Tarascani, *Polyhedron*, 26 (2007) 5150–5161.
8. S. Chandra and A. Rathi, *J. Saudi Chem. Soc.*, 5 (2001) 175–182.
9. N. Raman, A. Kulandaisamy, A. Shunmugasundaram and K. Jeyasubramanian, *Trans. Met. Chem.*, 26 (2001) 131–135.

10. N. Raman, A. Kulandaisamy and K. Jeyasubramanian, *Synth. React. Inorg. Metal-Org. Chem.*, 32 (2002) 1583–1610.
11. L. Singh, D. K. Sharma, U. Singh and A. Kumar, *Asian J. Chem.*, 16 (2004) 577–580.
12. N. Raman, C. Thangaraja and S. Johnsonraja, *Cent. Euro. J. Chem.*, 5 (2005) 537–555.
13. O. E. Offiong and S. Martelli, *Trans. Met. Chem.*, 22 (1997) 263–269.
14. E. Labisbal, K. D. Haslow, A. Sousa-Pedrares, J. Valdés-Martínez, S. Hernández-Ortega and D. X. West, *Polyhedron*, 22 (2003) 2831–2837.
15. K. Kumar, S. Schniper, A. González-Sarrías, A. A. Holder, N. Sanders, D. Sullivan, W. L. Jarrett, K. Davis, F. Bai, N. P. Seeram and V. Kumar, *Eur. J. Med. Chem.*, 86 (2014) 81–86.
16. S. B. Desai, P. B. Desai and K. R. Desai, *Commun*, 7 (2001) 83–90.
17. R. S. Kumar and S. Arunachalam, *Eur. J. Med. Chem.*, 44 (2009) 1878–1883.
18. J. Vanco, J. Marek, Z. Travnicek, E. Racanska, J. Muselik and O. Svajlenova, *J. Inorg. Biochem.*, 102 (2008) 595–605.
19. A. A. S. Al-Hamdani, A. M. Balkhi, A. Falah and S. A. Shaker, *J. Chil. Chem. Soc.*, 60 (2015) 2774–2785.
20. P. Brooks and N. Davidson, *J. Am. Chem. Soc.*, 82 (1960) 2118–2123.
21. M. Palanichamy and M. Anbu, *J. Chem. Sci.*, 109 (1997) 105–113.
22. V. R. Rajan, G. J. Pankaj and S. A. Sawant, *Asian J. Res. Chem.*, 5 (2012) 722–724.
23. G. H. Jaffery, J. Basset, J. Mendham and R. C. Denney, *Vogel's Textbook of Quantitative Chemical Analysis* 5th edition, Longman group, UK Limited, 1978.
24. A. Y. Hassan and H. A. Mohamed, *Asian J. Chem.*, 21 (2009) 3947–3961.
25. R. Hassanien, D. Z. Husein and M. F. Al-Hakkani, *Heliyon*, 4 (2018) e01077– e01097.
26. A. A. Al-Rashdi, A. H. Naggar, O. A. Farghaly, H. A. Mauof and A. A. Ekshiba, *Int. J. Electrochem. Sci.*, 14 (2019) 1132–1146.
27. G. A. Gouda and G. A. M. Ali, *Mal. J. Anal. Sci.*, 21 (2017) 1266–1275.
28. G. A. Gouda, T. A. Seaf-Elnasr, M. A. El-Mottaleb1 and A. Abd-Elmotagally, *J. Chem. Bio. Phy. Sci. Sec. A*, 7 (2017) 256–266.
29. H. M. Irving and H. S. Rossotti, *J. Chem. Soc.*, 75 (1953) 3397–3405.
30. H. M. Irving, M. G. Miles and L. D. Pettit, *Anal. Chim. Acta*, 38 (1967) 475–488.
31. H. Sari, M. Can and M. Macit, *Acta Chim. Slov.*, 52 (2005) 317–322.
32. M. B. Ferrari, S. Capacchi, G. Pelosi, G. Reffo, P. Tarasconi, R. Albertini, S. Pinelli and P. Lunghi, *Inorg. Chim. Acta*, 286 (1999) 134–141.
33. A. Castineiras, E. Bermejo, D. X. West, L. J. Ackerman, J. Valdes-Martinez and S. Hernandez-Ortega, *Polyhedron*, 18 (1999) 1463–1469.
34. Y. Altun, F. Koseoğlu, H. Demirelli, I. Ylmaz, A. Cukuroval and N. Kavak, *J. Braz. Chem. Soc.*, 20 (2009) 299–308.
35. Y. Altun and F. Köseoğlu, *Monat. Für. Chem.*, 137 (2006) 703–716.
36. M. M. Khalil, A. M. Radalla and A. G. Mohamed, *J. Chem. Eng. Data*, 54 (2009) 3261–3272.
37. L. T. Prakash, A. H. Gouri and T. N. Sharanappa, *J. Chem. Soc. Dalton Trans.*, 22 (1995) 3623–3626.
38. V. D. Athawale and V. Lelle, *J. Chem. Eng. Data*, 41 (1996) 1015–1019.
39. M. Magdy, K. Rehab and K. Mahmoud, *J. Saudi Chem. Soc.*, 20 (2016) 607–614.
40. R. Cornelis, J. Caruso, H. Crews and K. Heumann, *Handbook of Elemental Speciation: Techniques and Methodology* Wiley, New York (2003).
41. R. Thanavelan, G. Ramalingam, G. Manikandan and V. Thanikachalam, *J. Saudi Chem. Soc.*, 18 (2014) 227–233.
42. H. Irving and R. J. P. Williams, *J. Chem. Soc.*, 637 (1953) 3192–3210.
43. W. Andreas, M. A. Hitchman, W. Massa and D. Reinen, *Inorg. Chem.*, 32 (1993) 2483–2490.
44. G. A. Gouda, M. A. El-Mottaleb, N. A. Badawy, F. Kamale and SH. H. Ali, *Assiut Uni. J. Chem.*, 47 (2018) 51–65.

45. A. T. Mubarak, *J. Soln. Chem.*, 33 (2004) 1041–1048.
46. A. A. Amindzhanov, K. A. Manonov, N. G. Kabirov and G. A. H. Abdelrahman, *Rus. J. Inorg. Chem.*, 61 (2016) 81–85.
47. G. A. H. Gouda, G. A. M. Ali and T. A. Seaf-Elnasr, *Int. J. Nano. Chem.*, 1 (2015) 39–44.
48. B. S. Al-Farhan, G. A. Gouda, O. A. Farghaly and A. K. El-Khalafawy, *Int. J. Electrochem. Sci.*, 14 (2019) 3350–3362.
49. T. Ozer and I. Isildak, *Int. J. Electrochem. Sci.*, 13 (2018) 11375–11387.
50. L. H. Abdel-Rahman, A. M. Abu-Diefa, H. Moustafa and A. A. H. Abdel-Mawgouda, *Arab. J. Chem.*, 13 (2020) 649-670.
51. S. Chandra and S. A. Rathi, *J. Saudi Chem. Soc.*, 5 (2001) 175–182.
52. S. A. Aly and S. K. Fathalla, *Arab. J. Chem.*, 13 (2020) 3735-3750.
53. J. W. Bats, *Acta Crystallogr.*, 32 (1976) 2863–2866.
54. A. Gomez-Zavaglia, I. D. Reva, L. Frijia, M. L. Cristiano and R. Fausto, *J. Mol. Struct.*, 786 (2006) 182–192.
55. D. X. West and M. A. Lockwood, *Tran. Metal Chem.*, 18 (1993) 221–227.
56. U. Kumar and S. Chandra, *J. Saudi Chem. Soc.*, 15 (2011) 19–24.
57. X. Zhu, C. Wang, Z. Lu and Y. Dang, *Tran. Metal Chem.*, 22 (1997) 9–13.
58. B. Singh and H. Mishra, *J. Indian Chem. Soc.*, 63 (1986) 692–694.
59. E. Pahontu, V. Fala, A. Gulea, D. Poirier, V. Tapcov and T. Rosu, *Molecules*, 18 (2013) 8812–8836.
60. A. Becke, *Phys. Rev.*, 38 (1988) 3098–3100.
61. M. I. Elusta, M. A. Başaran and F. Kandemirli, *Int. J. Electrochem. Sci.*, 14 (2019) 2743–2756.
62. G. Gece, *Corr. Sci.*, 50 (2008) 2981–2992.